Electronic Supplementary Information for

Crystal structure dependent cation exchange reactions in $Cu_{2-x}S$ nanoparticles

Lihui Chen,[*a] Zhenzhen Kong,[b] Hengcong Tao,[a] Haifeng Hu,[b] Jing Gao[b] and Guohua Li[*b]

[a]*School of Petrochemical Engineering & Environment, Zhejiang Ocean University, No.1, Haida South Road, Lincheng Changzhi Island, Zhoushan 316022, China*

[b]*College of Chemical Engineering, Zhejiang University of Technology, 18, Chaowang Road, Hangzhou 310014, China*

Chemicals

Copper(I) chloride ($CuCl$, 99%), cadmium (II) chloride ($CdCl_2$, 99%), and 1-octadecene (ODE) were purchased from Sigma-Aldrich. Oleylamine (OAm, 80−90%) was purchased from Acros Organics. 1-dodecanethiol (1-DDT, 98%), crystal sulfur, trioctyl-phosphine (TOP, 98%), ethanol (99.5%), toluene, acetone, chloroform ($CHCl_3$) and other chemicals were purchased from Wako Chemicals. All the chemicals were used without any purification.

Characterizations

TEM observations were carried out using a JEM-1011 (JEOL) transmission electron microscope at an accelerating voltage of 100 kV. HRTEM and STEM images were obtained by using a TEM (Tecnai G2 F30 S-Twin, Philips-FEI, Netherlands) at an acceleration voltage of 300 kV. Elemental distribution/mapping was analyzed using energy dispersive X-ray spectroscopy (EDS) on a Tecnai G2 F30 equipped with an Oxford/INCA EDS. UV/vis/NIR (300 nm-2500 nm) absorption spectra of $Cu_{2-x}S$ NDs, CdS NDs, and the according heterostructures were measured in a 1 mm quartz cuvette using U-4100 spectrophotometer (HITACHI). The XRD patterns were taken on X'Pert Pro MPD (PANalytical) with CuKα radiation (λ = 1.542 Å) at 45 kV and 40 mA. X-ray fluorescence (XRF) analysis was examined with a JSX-3202C (JEOL) instrument at 30 kV and 1 mA. Raman spectra of $Cu_{2-x}S$ NDs and CdS NDs were recorded using inVia microscopic spectrometer (Renishaw). Data were obtained at λ = 532 nm with a 50× objective using a nominal power of 0.25 mW and integration time of 120 s.

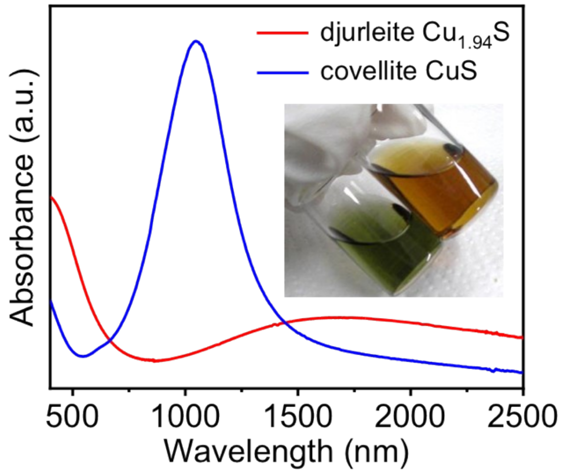

Figure S1. UV/vis/NIR absorption spectra of djurleite $Cu_{1.94}S$ NDs and covellite CuS NDs. Inset: digital photograph of $Cu_{1.94}S$ (brownish) and CuS (greenish) dispersed in $CHCl_3$.

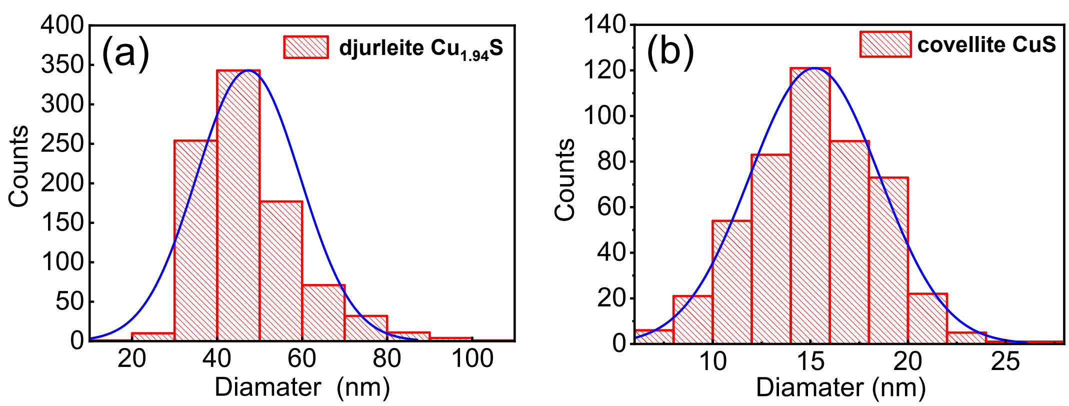

Figure S2. Size-distribution histograms of (a) djurleite $Cu_{1.94}S$ and (b) covellite CuS NDs.

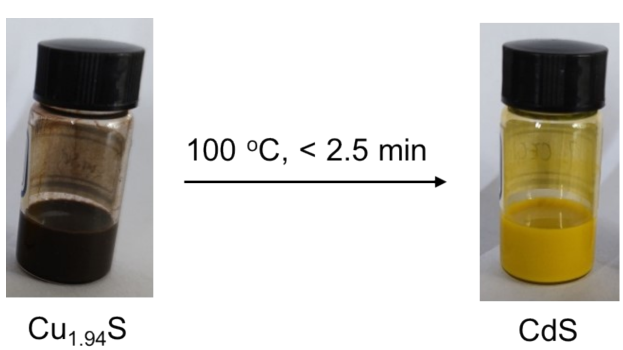

Figure S3. Rapid color change from $Cu_{1.94}S$ to CdS after full CE reaction.

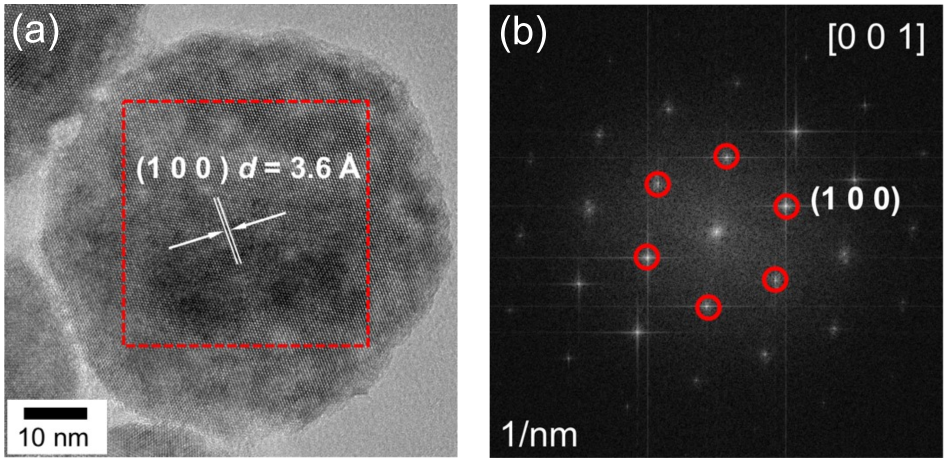

Figure S4. (a) HRTEM image of CdS NDs after full CE reaction from djurleite $Cu_{1.94}S$ ND. (b) Fast Fourier transform pattern of the CdS phase viewed from [0 0 1] direction.

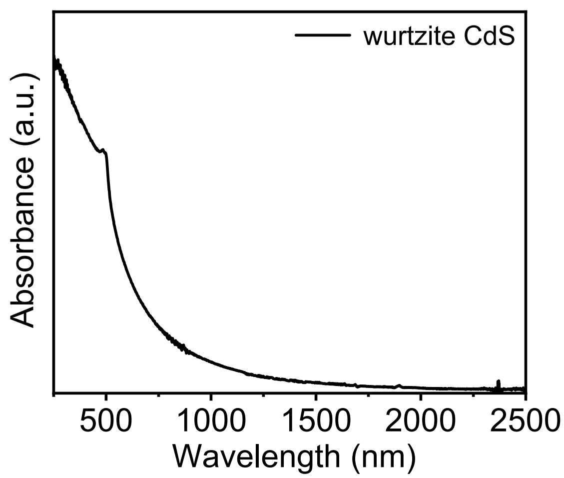

Figure S5. UV/vis/NIR absorption spectrum of the resulting CdS NDs. The absorption at longer wavelengths might be ascribed to the contribution from the residual Cu^+ in CdS NDs.

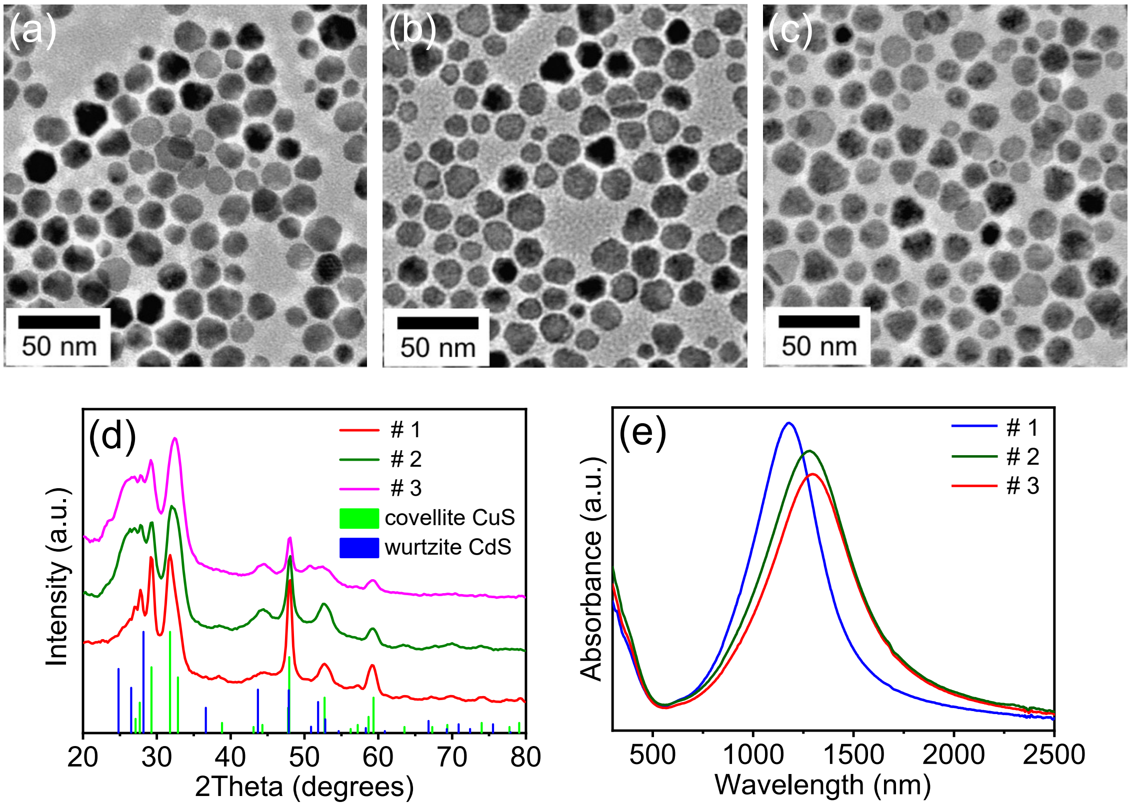

Figure S6. (a-c) TEM images of the resulting NDs obtained from CE reactions of covellite CuS with Cd^{2+}. Reaction condition for # 1: 0.5 mmol of CuS, 100 ^{o}C, 1.0 mmol of $CdCl_2$, 30 min; for # 2: 0.5 mmol of CuS, 100 ^{o}C, 1.0 mmol of $CdCl_2$, 180 min; for # 3: 0.5 mmol of CuS, 100 ^{o}C, 2.0 mmol of $CdCl_2$, 180 min. (d) XRD patterns and (e) UV/vis/NIR absorption spectra of the corresponding samples.

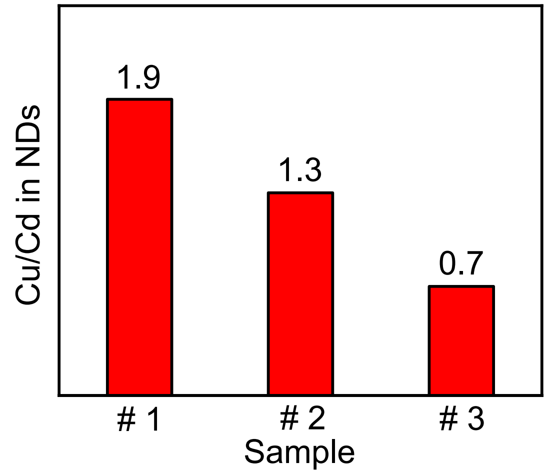

Figure S7. Cu/Cd molar ratio in # 1, # 2 and # 3 samples. Under the above reaction conditions, the Cu^{+} in the surface region of covellite CuS NDs is started to be expelled and the ND hosts the incoming Cd^{2+} perhaps through a surface adsorption process.

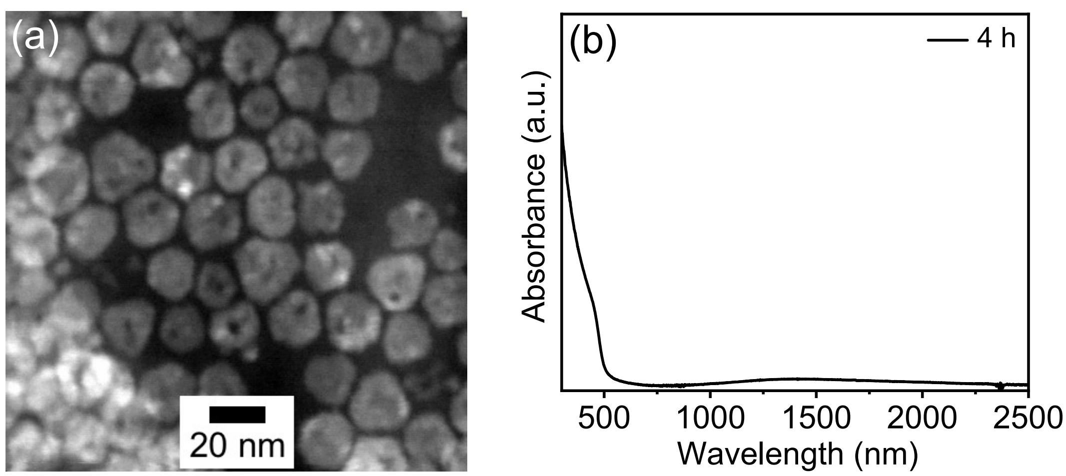

Figure S8. (a) Dark-field STEM image and (b) UV/vis/NIR absorption spectrum of the resulting CdS NDs obtained from CE reaction of covellite CuS with Cd^{2+} under the reaction condition: 0.5 mmol of CuS, 140 ^{o}C, 2.0 mmol of $CdCl_2$, 4 h.

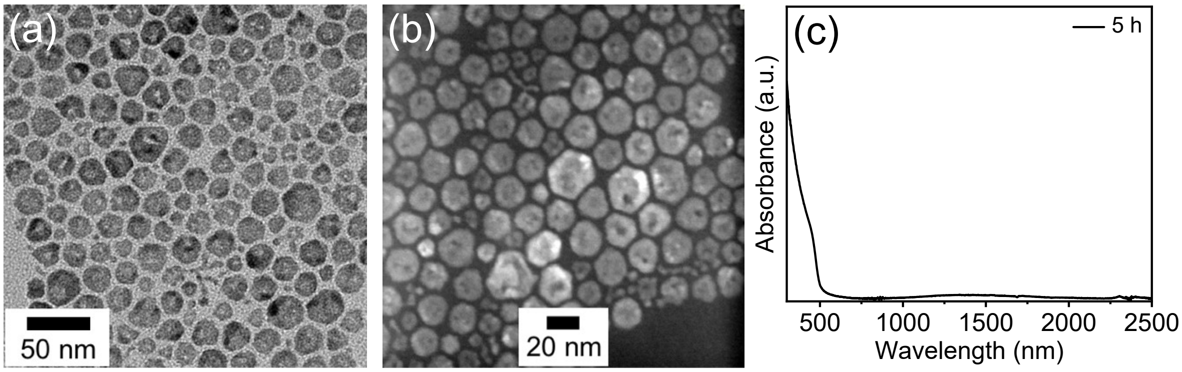

Figure S9. (a) Bright-field TEM image, (b) dark-field STEM image and (c) UV/vis/NIR absorption spectrum of the resulting CdS NDs obtained from CE reaction of covellite CuS with Cd^{2+} under the reaction condition: 0.5 mmol of CuS, 140 °C, 2.0 mmol of $CdCl_2$, 5 h.

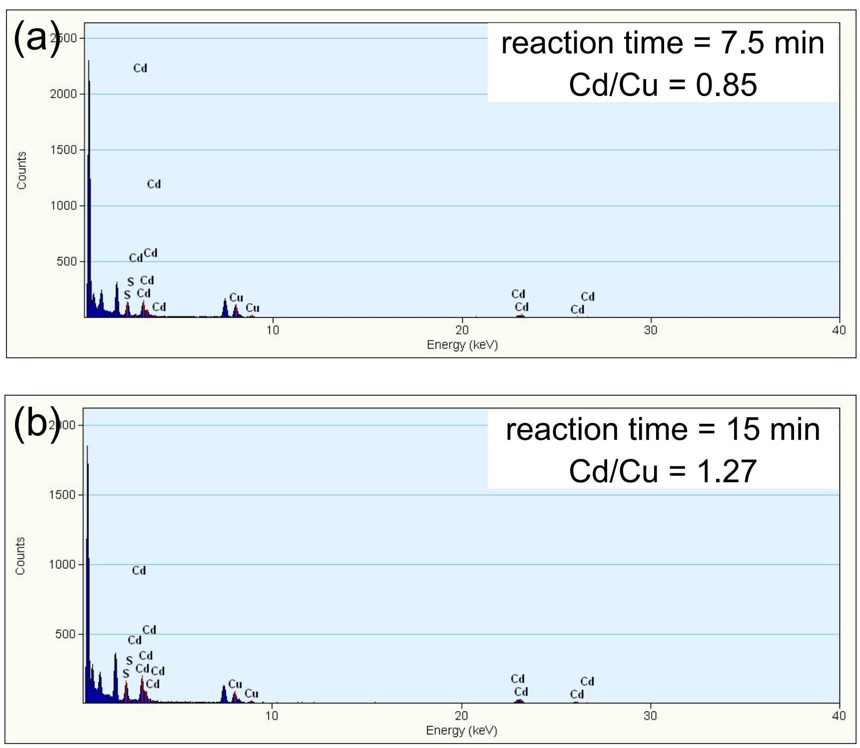

Figure S10. EDS spectrum of $Cu_{1.94}S$/CdS heterostructured NDs obtained under the reaction condition: $Cu_{1.94}S$ (containing 0.5 mmol Cu^{+}), 80 °C, 1.0 mmol of $CdCl_2$, (a) 7.5 min, and (b) 15 min.

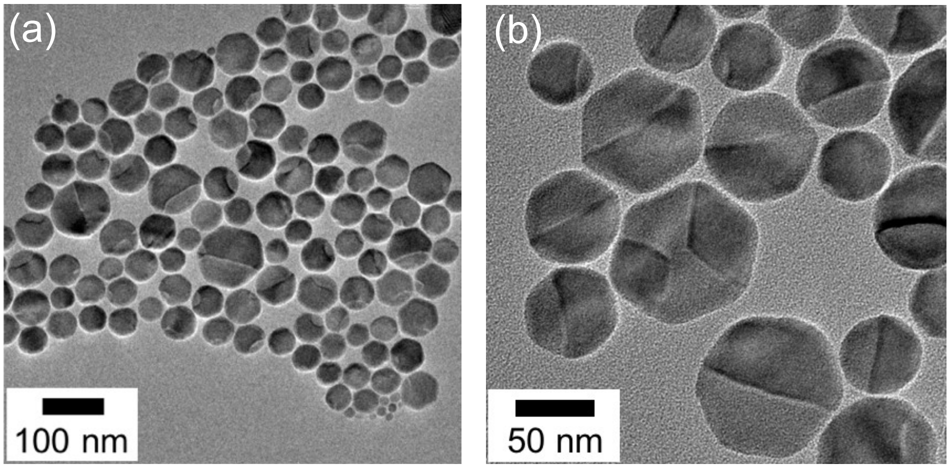

Figure S11. (a, b) Bright-field TEM images of $Cu_{1.94}S$/CdS NDs obtained under the reaction condition: $Cu_{1.94}S$ (containing 0.5 mmol Cu^{+}), 80 °C, 1.0 mmol of $CdCl_2$, 15 min.

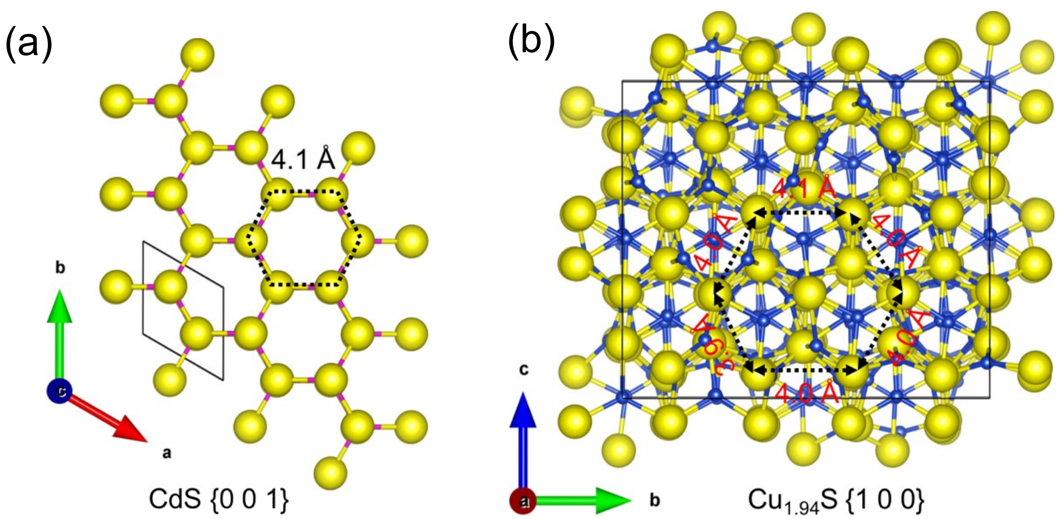

Figure S12. Distance between S-S sublayers in (a) CdS {0 0 1} and (b) $Cu_{1.94}S$ {1 0 0}. Yellow sphere: sulfur atom, pink sphere: cadmium atom, blue sphere: copper atom.

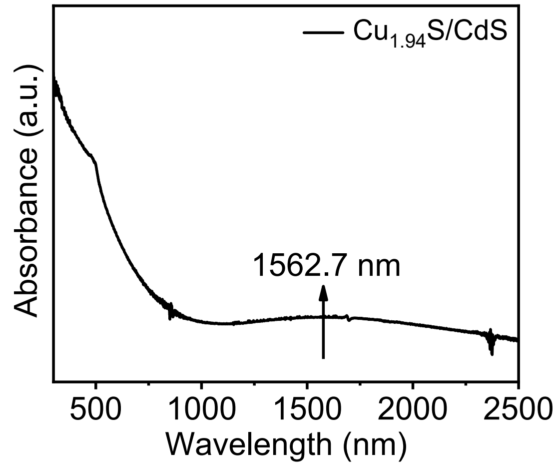

Figure S13. UV/vis/NIR absorption spectrum of $Cu_{1.94}S/CdS$ heterostructured NDs.

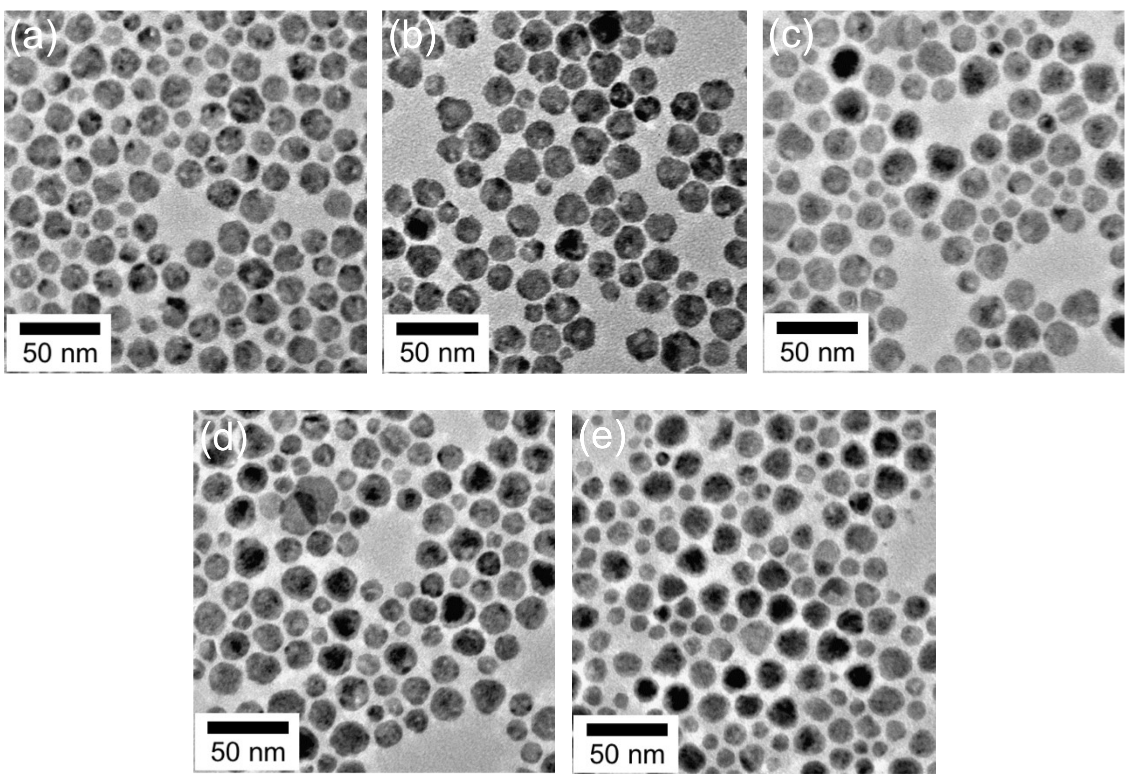

Figure S14. TEM images of the resulting CuS@CdS NDs obtained from CE reactions of CuS with Cd^{2+} under the reaction condition: 0.5 mmol of CuS, 140 °C, 2.0 mmol of $CdCl_2$ and the reaction time of (a) 180 min, (b) 60 min, (c) 40 min, (d) 20 min and (e) 10 min.

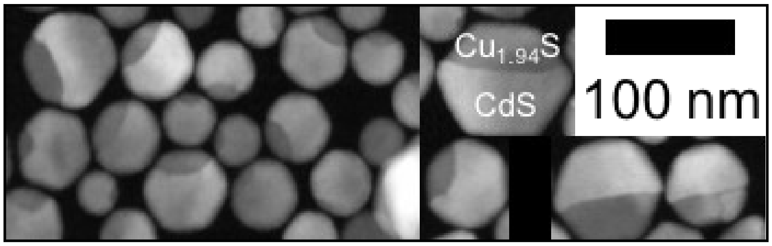

Figure S15. Dark-field STEM image of Janus-type $Cu_{1.94}S/CdS$ NDs. In spite of quite different particle size of starting $Cu_{1.94}S$ NDs, the formation of $Cu_{1.94}S/CdS$ is particle size independent and no core@shell nanostructure is observed.

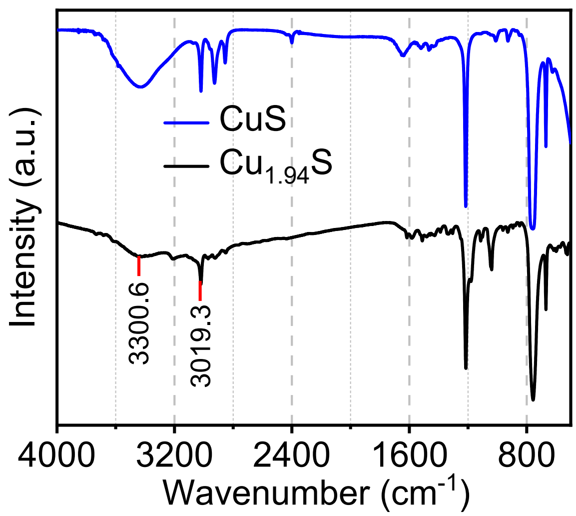

Figure S16. FTIR spectra of djurleite $Cu_{1.94}S$ NDs and covellite CuS NDs. The peak located at about 3300 cm^{-1}, 3019 cm^{-1} is assigned to $\nu_{as}(NH_2)/\nu_s(NH_2)$ and δ(=C-H), respectively. ν_{as} = asymmetric stretching vibration, ν_s = symmetric stretching vibration, and δ = bending vibration.

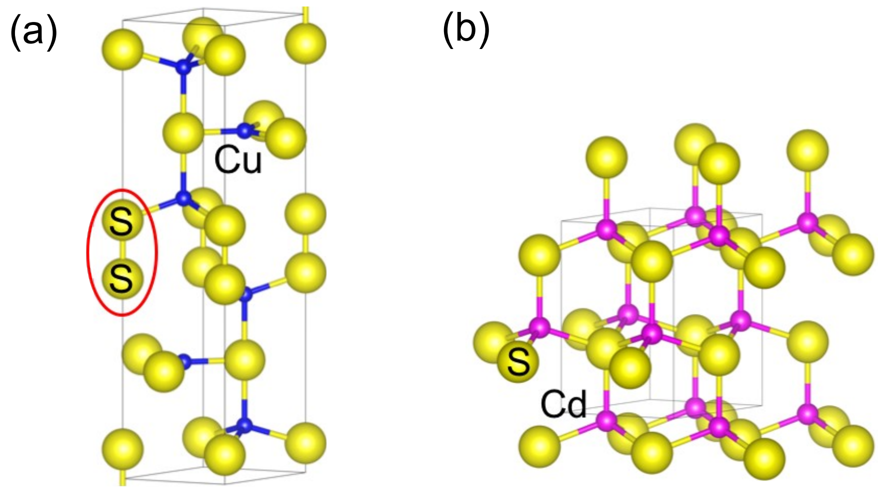

Figure S17. Unit cell of (a) covellite CuS and (b) wurtzite CdS.

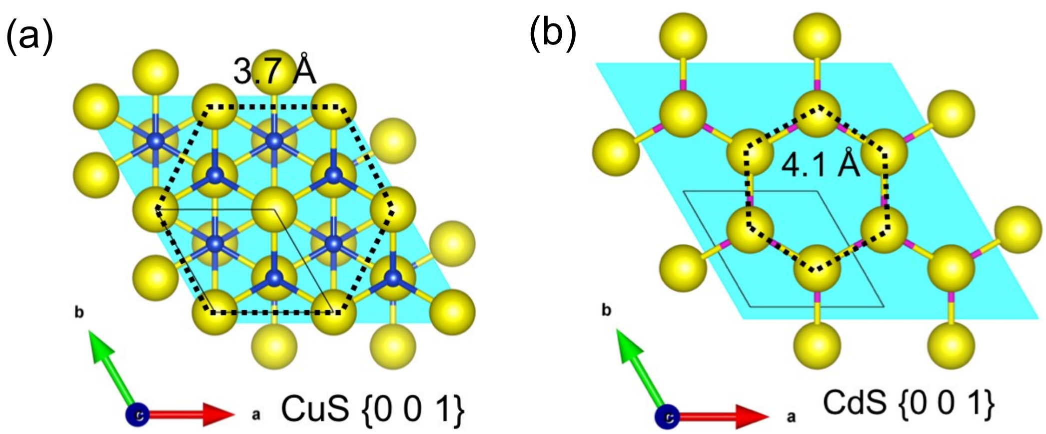

Figure 18. S-S distance in (a) CuS {0 0 1} and (b) CdS {0 0 1}. The mismatch of S-S distance in hexagonal sulfur sublattices is 9.8%. Yellow sphere: sulfur atom, pink sphere: cadmium atom, blue sphere: copper atom.